

# Silole-Containing Polyacetylenes. Synthesis, Thermal Stability, Light Emission, Nanodimensional Aggregation, and Restricted Intramolecular Rotation

Junwu Chen, Zhiliang Xie, Jacky W. Y. Lam, Charles C. W. Law, and Ben Zhong Tang\*

Department of Chemistry, Center for Display Research, Institute of Nano Science and Technology, and Open Laboratory of Chirotechnology of the Institute of Molecular Technology for Drug Discovery and Synthesis,<sup>†</sup> Hong Kong University of Science & Technology, Clear Water Bay, Kowloon, Hong Kong, China

Received August 19, 2002; Revised Manuscript Received December 10, 2002

**ABSTRACT:** We synthesized three substituted polyacetylenes carrying 1,2,3,4,5-pentaphenylsilyl (PS) pendants, i.e.,  $-\text{[HC=C(PS)]}_n-$  (**1**),  $-\text{[HC=C[(CH}_2)_9\text{OPS]}_n-$  (**2**) and  $-\text{[(C}_6\text{H}_5)_5\text{C=C[(CH}_2)_9\text{OPS]}_n-$  (**3**), and succeeded in turning polymers **2** and **3** from weak luminophors into strong emitters by external stimuli of aggregation and cooling. The silolylacetylene monomers  $\text{HC}\equiv\text{CPS}$  (**10**),  $\text{HC}\equiv\text{C(CH}_2)_9\text{OPS}$  (**11**), and  $\text{C}_6\text{H}_5\text{C}\equiv\text{C(CH}_2)_9\text{OPS}$  (**12**) were polymerized by  $\text{NbCl}_5-$  and  $\text{WCl}_6-\text{Ph}_4\text{Sn}$  catalysts, which gave high molecular weight polymers in high yields ( $M_w$  up to  $\sim 70 \times 10^3$  Da and yield up to  $\sim 80\%$ ). The structures and properties of the polymers were characterized and evaluated by IR, UV, NMR, DSC, TGA, PL, EL, and nanoparticle size analyses. The polymers were thermally stable and lost little weights when heated to  $\sim 350$  °C. Whereas all the polymers were practically nonluminescent when molecularly dissolved, polymers **2** and **3** became emissive when aggregated in poor solvents or when cooled to low temperatures. Restricted intramolecular rotation or twisting of the silole chromophores in the solid nanoaggregates or at the low temperatures may be responsible for the aggregation- or cooling-induced emission. A multilayer electroluminescence device using **3** as an active layer emitted a blue light of 496 nm with maximum brightness, current efficiency, and external quantum yield of 1118  $\text{cd/m}^2$ , 1.45  $\text{cd/A}$ , and 0.55%, respectively.

## Introduction

Silole is a five-membered silacycle, which may structurally be viewed as a cyclopentadiene derivative with its carbon bridge replaced by a silicon atom, hence the name silacyclopentadiene. Silole enjoys a unique  $\sigma^*-\pi^*$  conjugation arising from the orbital interaction of the  $\sigma^*$  orbital of its silylene moiety with the  $\pi^*$  orbital of its butadiene fragment, which significantly lowers its LUMO energy level and increases its electron affinity.<sup>1</sup> As a matter of fact, silole has the highest electron-accepting ability, in comparison to other conjugated five-membered heterocycles such as pyrrole, thiophene, and furan.<sup>2</sup> Thanks to its fast electron mobility,<sup>3</sup> silole has been used as an electron-transporting and light-emitting material in the construction of electroluminescence (EL) devices.<sup>4</sup>

We have recently observed an intriguing phenomenon of *aggregation-induced emission* (AIE) in a silole system.<sup>5</sup> 1-Methyl-1,2,3,4,5-pentaphenylsilole<sup>6</sup> (MPS, Chart 1) is practically nonluminescent in solutions but its films are highly emissive: the photoluminescence (PL) quantum yield ( $\Phi_{\text{PL}}$ ) of the silole aggregates can differ from that of its molecularly dissolved species by 2 orders of magnitude ( $>300$ ).<sup>5</sup> We fabricated a light-emitting diode (LED) using a thin solid film of MPS as an active layer, which luminesced strongly upon application of a low voltage. Its maximum current efficiency (CE) and power efficiency (PE) were 20  $\text{cd/A}$  and 14  $\text{lm/W}$ , respectively,

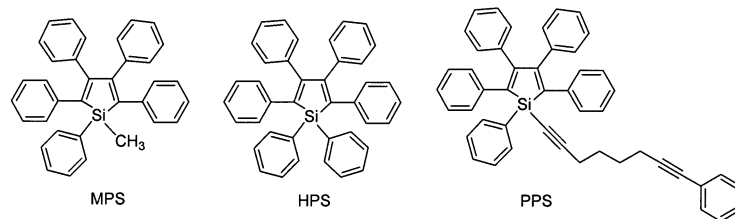
and its highest external quantum efficiency ( $\eta_{\text{EL}}$ ) was 8%,<sup>5,7</sup> approaching the limit of the possible.<sup>8,9</sup> An LED device of 1,1,2,3,4,5-hexaphenylsilole (HPS),<sup>6</sup> a structural congener of MPS, was turned on at a low voltage ( $\sim 4$  V), emitted intensely at a moderate bias (55 880  $\text{cd/m}^2$  at 16 V), and showed high EL efficiencies of 15  $\text{cd/A}$  (CE), 10  $\text{lm/W}$  (PE), and 7% ( $\eta_{\text{EL}}$ ).<sup>10</sup> An LED device of yet another silole compound, 1-(8-phenyl-1,7-octadiynyl)-1,2,3,4,5-pentaphenylsilole (PPS), also worked well and exhibited maximum EL efficiencies of 8.5  $\text{cd/A}$  (CE), 3.8  $\text{lm/W}$  (PE), and 3.9% ( $\eta_{\text{EL}}$ ). Similarly impressive device performances have been reported by other research groups for other silole molecules, examples of which include 2,5-bis(2,2'-bipyridin-6-yl)-1,1-dimethyl-3,4-diphenylsilole,<sup>3</sup> 1,2-bis(1-methyl-2,3,4,5-tetraphenylsilyl)ethane,<sup>3</sup> and dithienosilole and dithienodisilacyclohexadiene derivatives.<sup>11</sup>

Siloles are thus a group of excellent organometallic molecules for LED applications. Low molecular weight compounds, however, have to be fabricated into thin films by relatively expensive techniques such as vacuum sublimation and vapor deposition, which are not well suited to the manufacture of large area devices.<sup>12</sup> One way to overcome this processing disadvantage is to make high molecular weight polymers, which can be readily processed from their solutions into thin solid films over large areas by simple spin coating or doctor's blade techniques. Several research groups have worked on the preparation of silole-containing polymers.<sup>13</sup> Most of the methods used for the preparation of the silole polymers are based on polycoupling or polycondensation reactions. This method enjoys an advantage of versatility because of its "universal" applicability to multifunctional monomers: any pairs of monomers with two or

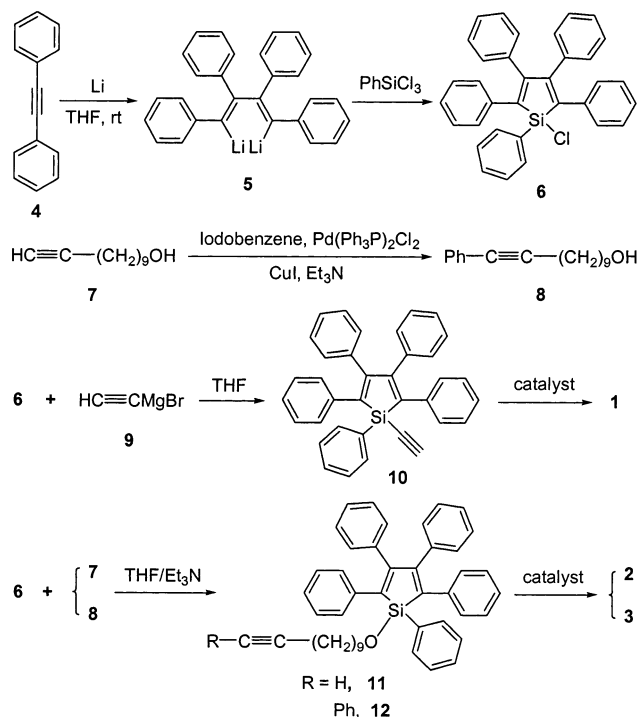
\* To whom all correspondence should be addressed at the Department of Chemistry, Hong Kong University of Science & Technology. Telephone: +852-2358-7375. Fax: +852-2358-1594. E-mail: tangbenz@ust.hk.

<sup>†</sup> An Area of Excellence (AoE) Scheme administrated by the University Grants Committee of Hong Kong.

Chart 1



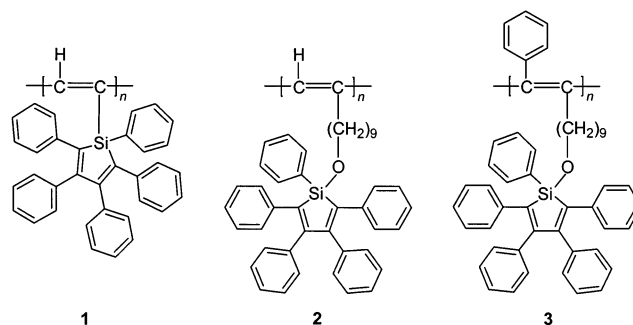
Scheme 1



more mutually reacting functional groups can, in principle, be polymerized by this reaction route. This synthetic route suffers, however, an operational disadvantage: it demands a stoichiometric balance of the monomer feed if one wishes to prepare a soluble polymer of high molecular weight. This technical difficulty has made the preparation of high molecular weight polysiloles a challenging task. Indeed, the polysiloles prepared by the polycondensation reactions have molecular weights normally on the order of  $10^3$  Da.<sup>13</sup>

In this work, we attempted to synthesize silole polymers through a different approach. We tried to knit the silole molecules together by a technique of acetylene metathesis polymerization,<sup>14</sup> which is, in terms of reaction mechanism, an addition or chain reaction but not a condensation or step reaction. To make the silole molecule metathesis-active, we attached an acetylene triple bond to the silolyl ring directly without a spacer (**10**, Scheme 1) or indirectly through a flexible nonanyl-oxy spacer (**11** and **12**). This structural design enables us to investigate the electronic communication of the polyacetylene backbone with the functional pendants and the effect of the flexible spacer on the interaction of the backbone with the pendants, both of which have been found to play important roles in the formation of mesomorphic aggregates in our liquid crystalline polyacetylene systems.<sup>15</sup> It is known that luminescence efficiency of a substituted polyacetylene carrying chromophoric pendants (Ch) varies significantly with its molecular structure: a monosubstituted poly(1-aryl-

Chart 2



acetylene)  $\{-[HC=C(Ar-Ch)]_n-\}$  is almost nonluminescent, a monosubstituted poly(1-alkyne)  $\{-[HC=C[(CH_2)_m-Ch]]_n-\}$  can be emissive, and a disubstituted poly(1-aryl-1-alkyne)  $\{-[ArC=C[(CH_2)_m-Ch]]_n-\}$  is often radiantly glowing.<sup>16</sup> We varied the substitution patterns of the silolylacetylene monomers, i.e., from monosubstituted 1-silolylacetylene (**10**) and  $\omega$ -silolyl-1-alkyne (**11**) to disubstituted 1-aryl-1-( $\omega$ -silolyl-1-alkyne) (**12**), in an effort to evaluate how the structural change will affect the light-emitting behaviors of the substituted polysilolylacetylenes (**1–3**, Chart 2).

Aggregation of conjugated polymer chains in the solid state often causes the formation of less-emissive or nonemissive species such as excimers and exciplexes, which partially or sometimes even completely quench the emission of the polymers.<sup>17</sup> This aggregation-induced quenching has been a thorny problem in the development of efficient LED systems because conjugated polymers are commonly used as thin solid films in the EL devices. In this regard, the AIE feature of the silole molecules is an invaluable property because aggregation is an inherent process accompanying film formation.<sup>18</sup> Will the silolylacetylene polymers still retain the AIE characteristics of their silole moieties or will their aggregates be emissive? How will the conjugated polyacetylene backbone affect the emission of the silole aggregates? What is the cause or mechanism for the AIE process? Can this process be controlled or tuned by simple external stimuli? In this paper, we will provide our answers to these questions.

## Experimental Section

The details about the reagents (materials), instrumentation procedures, device fabrications, monomer syntheses, and polymerization reactions are given in the Supporting Information, in which the detailed characterization data for all the new monomers and polymers, including their isolation yields, physical forms (colors), molecular weights, and spectroscopic data (IR, <sup>1</sup>H and <sup>13</sup>C NMR, MS, and UV) are also listed.

## Results and Discussion

**Monomer Synthesis.** We synthesized three silolyl-acetylenes (**10–12**) by nucleophilic substitutions of 1-chloro-1,2,3,4,5-pentaphenylsilole (**6**) with a Grignard

reagent of ethynylmagnesium bromide (**9**)<sup>13f</sup> and two alkyne alcohols (**7** and **8**, Scheme 1). The chlorosilole **6** is an important intermediate for silole derivatizations, whose synthesis has, however, been difficult. Curtis prepared the compound<sup>19</sup> according to Braye's procedure<sup>20</sup> by first reacting toluene (**4**) with an excessive amount of lithium metal and then treating the resultant 1,4-dilithiotetraphenylbutadiene (**5**) with trichlorophenylsilane. This synthetic route has, however, several drawbacks. The use of an excess amount of lithium in the preparation of **5** can easily cause side reactions, leading to the formation of byproducts such as 1,2,3-triphenyl-naphthalene, as signaled by the color change of the reaction mixture from dark green to brownish-violet when the reaction time is prolonged.<sup>20</sup> To avoid the side reactions, a short reaction time is necessary (<2 h as advised by Curtis<sup>19</sup>); doing so, however, results in a low conversion of toluene to **5**. The existence of the unreacted lithium metal in the reaction mixture can cause further complications when the mixture is added into a chlorosilane solution. Gilman et al. thus recommended that excessive lithium should be carefully avoided even in the reactions of **5** with dichlorosilanes,<sup>21</sup> not to mention its reactions with trichlorosilanes.

We followed Curtis' procedure but encountered great difficulty in obtaining our desired products. We thus modified the reaction procedure and used an excessive amount of toluene, instead of lithium, in the preparation of **5**. This allowed the lithiation reaction to be carried out in an extended time frame to afford **5** in a high yield (~90%; estimated by a quenching reaction of **5** by water<sup>6</sup>). Little, if any, lithium metal was left in the mixture, and the side reactions were thus suppressed. The green color of the reaction mixture did not change for as long as 18 h, so the solution of **5** could be added with ease in a dropwise fashion to the phenyltrichlorosilane solution. After the addition, the mixture was allowed to reflux for 3–5 h, which gave a dark yellow solution of chlorosilole intermediate **6**. Upon cooling to room temperature, the chlorosilole was readily transformed to 1,2,3,4,5-pentaphenylsilolylacetylene (**10**), 11-[(1,2,3,4,5-pentaphenylsilolyl)oxy]-1-undecyne (**11**), and 11-[(1,2,3,4,5-pentaphenylsilolyl)oxy]-1-phenyl-1-undecyne (**12**) by the reactions with ethynylmagnesium bromide (**9**), 10-undecyn-1-ol (**7**), and 11-phenyl-10-undecyn-1-ol (**8**), respectively. The unreacted toluene was easily separated from the silole products by column chromatography<sup>22</sup> and could be recycled or reused. Monomers **10–12** were prepared in 25–35% yields, based on the amount of trichlorophenylsilane used, which were far better than what we could achieve with the Curtis procedure. All the purified monomers were fully characterized by standard spectroscopic methods, from which, satisfactory analysis data corresponding to their expected molecular structures were obtained (see Supporting Information for details). Single-crystal analysis of monomer **10** revealed that the silolylacetylene molecules were packed in a regular columnar structure, details of which will be published in a separate paper.<sup>23</sup>

**Polymerization Reactions.** Silolylacetylene **10**, a monomer with the silolyl moiety directly attached to the acetylene triple bond without a spacer, showed interesting polymerization behaviors. Since **10** structurally somewhat resembles phenylacetylene, we first tried to polymerize it by [Rh(nbd)Cl]<sub>2</sub>, an effective catalyst for the insertion polymerizations of phenylacetylenes.<sup>24,25</sup> The reaction catalyzed by the Rh complex in THF/Et<sub>3</sub>N,

**Table 1. Polymerization of Silolylacetylene **10**<sup>a,b</sup>**

no.	catalyst	solvent	temp (°C)	yield (%)	<i>M<sub>w</sub></i> <sup>c</sup>	<i>M<sub>w</sub></i> / <i>M<sub>n</sub></i> <sup>c</sup>
1	[Rh(nbd)Cl] <sub>2</sub>	THF/Et <sub>3</sub> N	rt	0		
2	WCl <sub>6</sub> -Ph <sub>4</sub> Sn	toluene	60	0		
3	MoCl <sub>5</sub> -Ph <sub>4</sub> Sn	toluene	60	0		
4	TaCl <sub>5</sub> -Ph <sub>4</sub> Sn	toluene	60	0		
5	NbCl <sub>5</sub> -Ph <sub>4</sub> Sn	toluene	60	60.0	46 400	1.7
6	NbCl <sub>5</sub> -Ph <sub>4</sub> Sn	toluene	80	78.0	68 800	1.8

<sup>a</sup> Carried out under nitrogen for 24 h; [M]<sub>0</sub> = 0.1 M; [cat.] = [cocat.] = 10 mM. <sup>b</sup> Abbreviations: nbd = 2,5-norbornadiene; rt = room temperature. <sup>c</sup> Estimated by GPC in THF on the basis of a polystyrene calibration.

however, yielded no polymeric product (Table 1, no. 1). Changing the solvent to dichloromethane (DCM) did not help. Disappointed by the Rh results, we turned our attention to metathesis catalysts. The mixtures of WCl<sub>6</sub>- and MoCl<sub>5</sub>-Ph<sub>4</sub>Sn are known to be active catalysts for the metathesis polymerizations of silicon-containing acetylenes of general structure HC≡C-SiMe<sub>2</sub>R.<sup>26,27</sup> Neither the W nor the Mo mixtures were, however, capable of polymerizing **10**. Attachment of the bulky silole group to the triple bond may have lowered the polymerizability of the acetylene monomer, preventing it from being polymerized by the W and Mo catalysts. The TaCl<sub>5</sub>- and NbCl<sub>5</sub>-Ph<sub>4</sub>Sn mixtures are known to be more tolerant of bulky groups and can polymerize sterically very crowded diphenylacetylene derivatives such as 1-phenyl-2-[(*p*-triphenylsilyl)phenyl]acetylene.<sup>27</sup> Unfortunately, our attempt to polymerize **10** by TaCl<sub>5</sub>-Ph<sub>4</sub>Sn mixture also failed. Delightfully, however, the reaction catalyzed by NbCl<sub>5</sub>-Ph<sub>4</sub>Sn in toluene at 60 °C produced red powdery polymer in a satisfactory yield (60%; Table 1, no. 5). The polymerization proceeded even more smoothly at a higher temperature (80 °C) and a polymer with a molecular weight of ~69 kDa was obtained in a high yield (78%). Monosubstituted acetylenes normally undergo cyclotrimerizations in the presence of NbCl<sub>5</sub>-Ph<sub>4</sub>Sn mixture,<sup>27,28</sup> and the polymerization of **10**, a monosubstituted acetylene, into high molecular weight polymers by the Nb catalyst is thus somewhat surprising. While a couple of silicon-containing alkynes and phenylacetylenes have been polymerized by NbCl<sub>5</sub>-Ph<sub>4</sub>Sn,<sup>29</sup> **10** is the first example of a monosubstituted silylacetylene with the silicon atom directly attached to the triple bond that can be successfully polymerized by the Nb catalyst. While poly(trimethylsilylacetylene), -{HC≡C[Si(CH<sub>3</sub>)<sub>3</sub>]}<sub>n</sub>-, is only partially soluble,<sup>26,27</sup> the polymers of **10** were completely soluble in common solvents such as chloroform, DCM, toluene, THF, and dioxane. The excellent solubility is probably due to the large free volumes created by the bulky silolyl pendants.

The polymerization behaviors of **11**, a monomer with the silolyl moiety separated from the triple bond by a long nonanyloxy spacer, were distinctly different from that of **10**. While WCl<sub>6</sub>-Ph<sub>4</sub>Sn was inactive in polymerizing **10**, the W catalyst effectively initiated the polymerization of **11** in toluene at 60 °C (Table 2, no. 1), giving a polymer with an *M<sub>w</sub>* of ~12 kDa in ~60% yield. The polymerization in dioxane proceeded to produce a high molecular weight polymer, albeit in a low yield. The polymerization was initiated by MoCl<sub>5</sub>-Ph<sub>4</sub>Sn catalyst but the result was much poorer than those from the W system. Like **11**, **12** was also polymerized by WCl<sub>6</sub>-Ph<sub>4</sub>Sn, giving a polymer with a high molecular weight (~33 kDa) in a high yield (~80%). Our attempts to polymerize

**Table 2. Polymerization of Siloxyacetylenes 11 and 12<sup>a</sup>**

no.	monomer	catalyst	solvent	yield (%)	$M_w^b$	$M_w/M_n^b$
1	<b>11</b>	WCl <sub>6</sub> -Ph <sub>4</sub> Sn	toluene	60.3	11 500	3.5
2	<b>11</b>	WCl <sub>6</sub> -Ph <sub>4</sub> Sn	dioxane	29.0	33 900	2.6
3	<b>11</b>	MoCl <sub>5</sub> -Ph <sub>4</sub> Sn	toluene	11.7	10 600	3.4
4	<b>12</b>	WCl <sub>6</sub> -Ph <sub>4</sub> Sn	toluene	80.5	33 400	2.2
5	<b>12</b>	TaCl <sub>5</sub> -Ph <sub>4</sub> Sn	toluene	0		
6	<b>12</b>	NbCl <sub>5</sub> -Ph <sub>4</sub> Sn	toluene	0		

<sup>a</sup> Carried out under nitrogen at 60 °C for 24 h; [M]<sub>0</sub> = 0.1 M; [cat.] = [cocat.] = 10 mM. <sup>b</sup> Estimated by GPC in THF on the basis of a polystyrene calibration.

**12** by TaCl<sub>5</sub>- and NbCl<sub>5</sub>-Ph<sub>4</sub>Sn catalysts were, however, unsuccessful. The polymerizations of the acetylene monomers with siloxy (Si-O) moieties (or siloxyacetylenes) seemed to be sensitive to not only the catalyst but also the substrate. We tried, for example, to polymerize a congener of **12** with a short ethyloxy spacer HC≡C(CH<sub>2</sub>)<sub>2</sub>OPS using the W and Mo catalysts under various reaction conditions, but our efforts all ended in failure. This may account for the rarity of reports on the polymerizations of siloxyacetylenes in the literature.<sup>27</sup> The only example known to us is the MoCl<sub>5</sub>-catalyzed polymerizations of dimethylalkoxysilylacetylenes HC≡CSi(CH<sub>3</sub>)<sub>2</sub>OC<sub>m</sub>H<sub>2m+1</sub> (*m* = 2, 3), which gave insoluble gels of low stability.<sup>26a</sup> The intractability not only poses an obstacle to purifying and characterizing the polymers but also renders the polymers practically useless in terms of finding practical applications as plastic materials. The polymers of **11** and **12** were, however, completely soluble in common organic solvents. These polymers thus represent the first examples of completely soluble substituted polyacetylenes with polar siloxy moieties.

**Structural Characterization.** All the polymers gave satisfactory spectroscopic data corresponding to their expected molecular structures (see Supporting Information for detailed analysis data). An example of the IR spectrum of polymer **2** is shown in Figure s1 (Supporting Information); the spectrum of its monomer **11** is also shown in the same figure for the purpose of comparison. As can be seen from the spectrum of **11**, its ≡C-H stretching and C=C bending vibrations occurred at 3297 and 637 cm<sup>-1</sup>, respectively.<sup>16a</sup> These absorption bands disappeared in the spectrum of its polymer, **2**, indicating that the triple bond has been consumed by the polymerization reaction.

The NMR analysis proved that the acetylene triple bonds had been transformed to polyene double bonds. Figure 1 shows the <sup>1</sup>H NMR spectra of **11** and its polymer **2** in CDCl<sub>3</sub>. There was no acetylene absorption at δ 1.9 in the spectrum of the polymer. It is known that the cis olefin proton of the poly(1-alkyne) backbone absorbs at δ 6.5–5.6.<sup>14–16</sup> The spectrum of **2**, however, exhibited no resonance peak in this region, suggesting that the polymer chains are *trans*-rich in stereostructure. Figure s2 (Supporting Information) shows the <sup>13</sup>C NMR spectra of the polymer and its monomer. While the acetylenic carbon atoms of **11** absorbed at δ 84.7 and 68.1, these absorption peaks disappeared in the spectrum of **2**. The absorption of the propargyl carbon atom of **11** at δ 18.4 also disappeared owing to its transformation to the allylic structure by the acetylene polymerization.<sup>16a</sup> The absorption peaks of the olefinic carbon atoms of the polyacetylene backbone were not easily identifiable, due to their overlapping with the resonance peaks of the silole pendants.

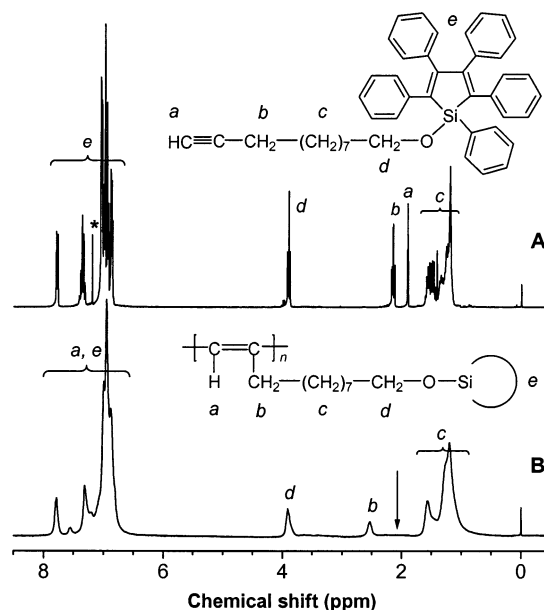


**Figure 1.** <sup>1</sup>H NMR spectra of (A) **11** and (B) its polymer **2** (Table 2, no. 1) in CDCl<sub>3</sub>. The solvent peak is marked with an asterisk. The silolyl moiety in the molecular structure of the polymer is represented by an Si ring in order to save space.

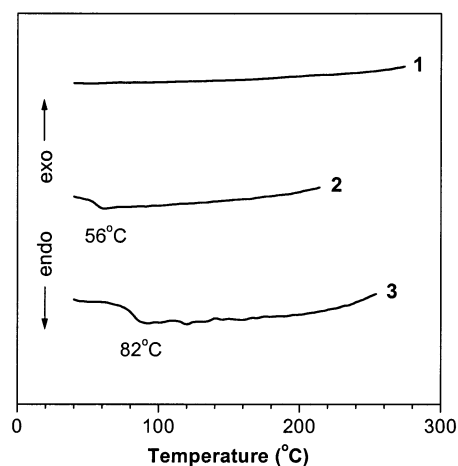


**Figure 2.** DSC thermograms of **1** (Table 1, no. 6), **2** (Table 2, no. 1), and **3** (Table 2, no. 4) recorded under nitrogen at a heating rate of 10 °C/min.

**Thermal Properties.** Figure 2 shows the DSC thermograms of polymers **1–3**. No peaks associated with crystallization/melting transitions of the polymers were detected by the DSC analyses. The glass transition temperatures (*T*<sub>g</sub>'s) of **2** and **3** were observed at 56 and 82 °C, respectively, while **1** exhibited a virtually flat line with no changes in the measured temperature region, suggesting that this polymer has a very high *T*<sub>g</sub>. The bulky pentaphenylsilolyl pendants directly attached to the polyacetylene backbone make the polymer chain very rigid, whose segmental movements are significantly restricted and cannot occur at low temperatures. The higher *T*<sub>g</sub> of **3**, in comparison to that of **2**, should be due to its more rigid disubstituted polyacetylene backbone.<sup>30</sup>

The TGA thermograms of the polymers are shown in Figure s3 (Supporting Information). All the polymers were thermally stable and lost little of their weights at a temperature as high as ~350 °C. The decomposition temperatures for poly(dimethylalkoxysilylacetylenes) -{HC=C[Si(CH<sub>3</sub>)<sub>2</sub>OC<sub>m</sub>H<sub>2m+1</sub>]}<sub>n</sub>- are 280 (*m* = 2) and

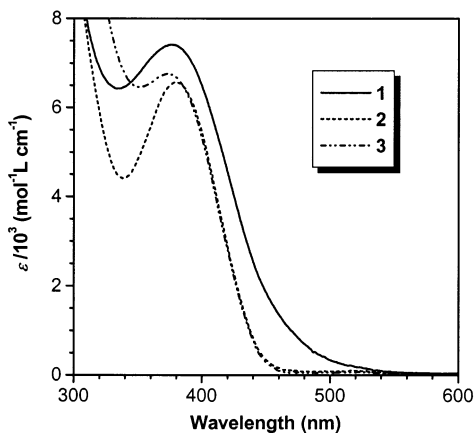


**Figure 3.** UV absorption spectra of chloroform solutions of **1** (Table 1, no. 6), **2** (Table 2, no. 1), and **3** (Table 2, no. 4).

270 °C ( $m = 3$ ), respectively;<sup>26a</sup> the higher stability of our polysilyloxyacetylenes **2** and **3** are probably due to the “jacket effect”<sup>15,16</sup> of the bulky silolyl pendants. Wrapping of the polyacetylene backbone in the silole rings may have shielded the double bonds from the chemical and thermal attacks. It has been reported that the siloxy bonds have been cleaved during the  $\text{MoCl}_5$ -catalyzed polymerizations of dimethylalkoxysilylacetylenes.<sup>26a</sup> Such detrimental cleavage reaction did not occur in the polymerizations of our sililyloxyacetylene monomers **11** and **12**, demonstrative of the multifaceted protective functions of the bulky silole rings.

**Electronic Transitions.** Polymer **1** exhibited a strong peak at 376 nm due to the absorption of its silole pendants, and the absorption of its polyacetylene backbone occurred at wavelengths beyond 450 nm, which well extended into the visible spectral region (Figure 3). The silole pendants may have conjugated with the polyacetylene backbone, which increased the effective conjugation length of the polymer chain,<sup>31</sup> hence making the polymer absorptive in the long wavelength region.<sup>32</sup> Little absorption was, however, observed in the long wavelength region of the spectra of **2** and **3**, suggesting that these polymers possess shorter persistence lengths of backbone conjugations, in comparison to their structural congener **1**. This difference was reflected in the colors of the polymers: while **1** was red-colored, **2** and **3** were yellow-greenish solids. Compared to **2**, **3** absorbed more strongly in the short wavelength region (<380 nm). This enhanced absorption is probably due to the additional contribution from the phenyl rings directly attached to the polymer backbone.

Figure 4 shows the absorption spectra of the polymers in methanol/chloroform mixtures. The mixtures were prepared by adding methanol into dilute chloroform solutions of the polymers with vigorous shaking, the concentrations of all the resultant mixtures being kept fixed at 10  $\mu\text{M}$  for the purpose of comparison. One can immediately notice, by comparing the spectra in Figure 4, that there are practically no shifts in the peak positions for all the three polymers, no matter how the solvent composition changes. The absorptivity of the mixtures, however, did change, although in a mixed manner. With an increase in methanol content in the mixture, the spectrum of **1** was vertically lifted up, little change was observed in the absorption spectra of **2**, and the spectra of **3** was somewhat elevated. What is the cause for this kind of spectral variation? Nanoparticles are known to vertically raise absorption spectra due to

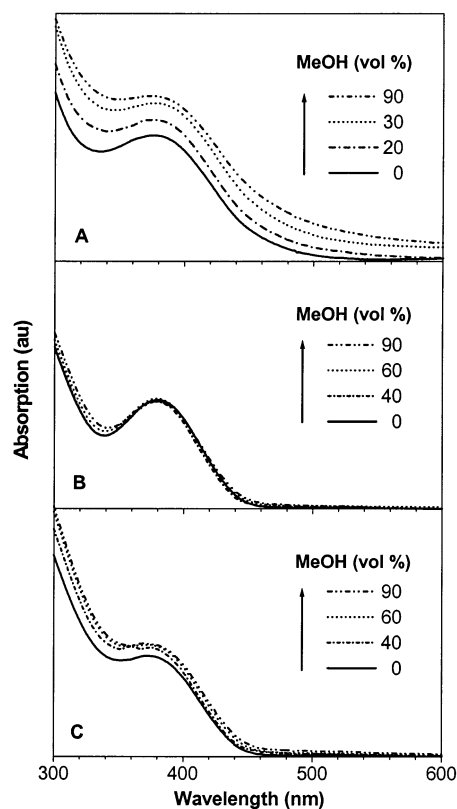


**Figure 4.** Absorption spectra of (A) **1** (Table 1, no. 6), (B) **2** (Table 2, no. 1), and (C) **3** (Table 2, no. 4) in methanol/chloroform mixtures with different volume fractions of methanol.

the optical loss caused by light scattering.<sup>33,34</sup> Since methanol is a poor solvent of the polymers, it is likely that the polymers have formed nanosized aggregates in the methanol/chloroform mixtures with high contents of methanol. We thus checked whether there were really nanoparticles in such mixtures.

We carried out particle size analysis, which proved that the polymers did form nanoaggregates in the methanol/chloroform mixtures. Examples of the particle size histograms are shown in Figure 5. In the mixture with 90% methanol, **1** clustered into large particles with a broad size distribution and a large average size (174 nm). Polymer **2** also formed nanoaggregates, whose size distribution was, however, much narrower and whose average size was much smaller (34 nm). The size distribution and average size (112 nm) of **3** were between those of **1** and **2**. The differences in the size distribution and average size are probably due to the difference in the solubility of the polymers in the solvent mixture. Polymer **1** is very hydrophobic and rigid and will easily associate into large nanoaggregates in the polar mixture. Polymer **2** possesses polar siloxy moieties with a better miscibility with the polar solvent and hence forms smaller aggregates under comparable conditions. Polymer **3** is a disubstituted polyacetylene with a more rigid backbone structure<sup>30</sup> and its aggregates are thus understandably bigger than those of **2**. With the nanoparticle data on hand, we now may understand why the absorption spectra of the polymers have changed in a seemingly confusing manner with the progressive addition of methanol into the chloroform solutions. The formation of nanoaggregates may have not appreciably perturbed the electronic structures of the polymers and has hence caused practically no red

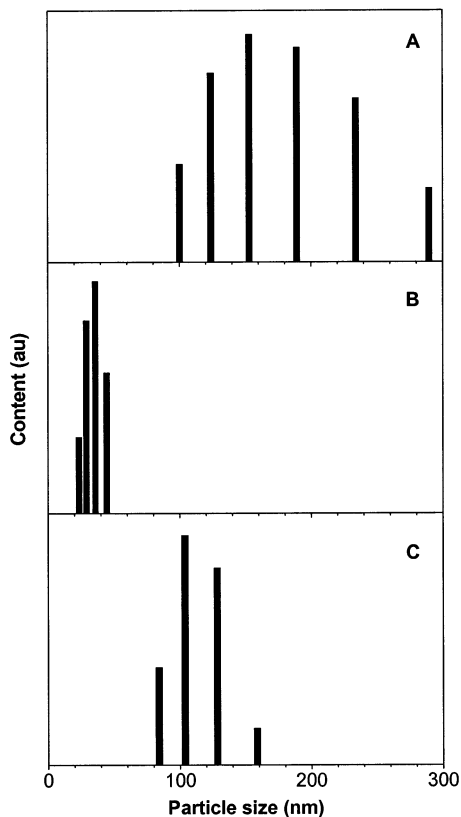


**Figure 5.** Particle size distributions of (A) **1** (Table 1, no. 6), (B) **2** (Table 2, no. 1), and (C) **3** (Table 2, no. 4) in methanol/chloroform mixtures (9:1 by volume). Concentration of polymers: 10  $\mu$ M.

shifts in the peak positions of their absorption spectra. The optical losses caused by the light scattering from the nanoparticles of **1** and **3** vertically upraise the levels of spectra, albeit in a nonlinear fashion due partly to the size distribution of the nanoparticles.<sup>33</sup> The sizes of the nanoparticles of **2** are too small to induce noticeable scattering loss,<sup>35</sup> and hence, its spectra did not change much with the solvent composition.

**Light Emission.** Silole's emission is characterized by its AIE feature:<sup>5</sup> it is practically nonluminescent when molecularly dissolved in solutions but is highly emissive when aggregated in poor solvents or fabricated into thin solid films. Do the silole polymers behave in a similar way? The answer to this question is yes or no, depending on the molecular structure of the polymer. A chloroform solution of **1** with a concentration of 10  $\mu$ M emitted a faint red light of 652 nm. It is known that the silole ring emits blue-green light<sup>5-8</sup> while the (unsubstituted) polyacetylene chain emits weak infrared light.<sup>36</sup> The emission of the dim red light of 652 nm thus should be associated with the inefficient radiative decay of the somewhat twisted polyacetylene backbone of **1**. We added methanol into the chloroform solution, while keeping the concentrations of the resultant mixtures unchanged. Only very slightly could the light emission of **1** be enhanced by the addition of the poor solvent; that is, this polymer does not show the AIE effect.

Polymer **2**, on the other hand, exhibited a pronounced AIE effect. While the PL spectrum of its dilute chloroform solution was almost a flat line, intense emission was observed when a large amount (90 vol %) of methanol was added into the chloroform solution (Figure S4A, Supporting Information). Its thin solid film was also highly emissive. The emission peaks of the methanol/

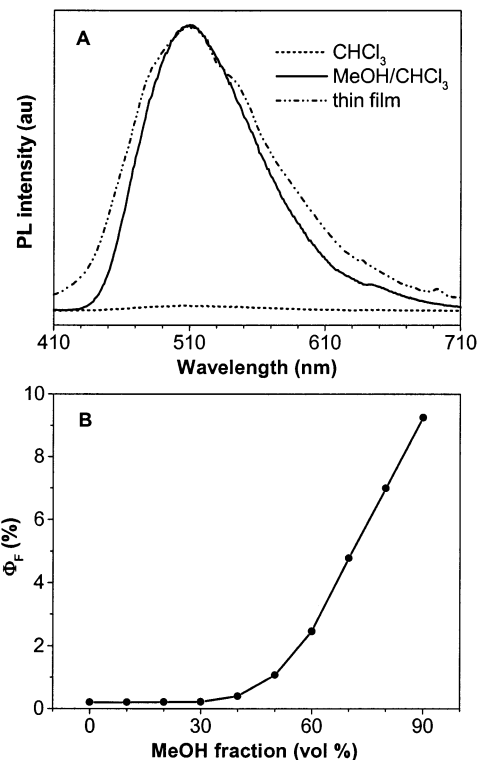


**Figure 6.** (A) Photoluminescence spectra of **3** (Table 2, no. 4) in chloroform solution, methanol/chloroform mixture (9:1 by volume), and solid state (thin film). Concentration of **3** in the solution and the mixture: 10  $\mu$ M. Excitation wavelength (nm): 400 (solution/mixture); 325 (thin film). (B) Quantum yield ( $\Phi_F$ ) of **3** vs solvent composition of methanol/chloroform mixture.

chloroform mixture and the thin film both located at 512 nm, which is close to the emission maximum of the silole ring, suggesting that the emission of **2** is by its silole pendants. We estimated the quantum yield ( $\Phi_F$ ) of **2** using 9,10-diphenylanthracene as reference.<sup>5</sup> Its chloroform solution showed a  $\Phi_F$  value as low as 0.15%. The  $\Phi_F$  value of the mixture remained almost unchanged when up to ~40% methanol was added to the solution but started to swiftly increase afterward (Figure 4B). When the methanol fraction was increased to 90%,  $\Phi_F$  rose to 2.95%, which was ~20 times higher than the solution value. The trajectory of the  $\Phi_F$  change suggests that the silole pendants of **2** started to aggregate at a methanol fraction of ~50% and that the size and population of the nanoaggregates continue to increase as the methanol fraction increases. Similarly, polymer **3** was also AIE-active: its solution was almost nonradiative, but its aggregates luminesced intensely at 512 nm (Figure 6A). The emission efficiency of **3** ( $\Phi_F = 9.25\%$ ) was >3 times higher than that of **2**, probably due to the additional contribution of the backbone emission: the poly(1-phenyl-1-alkyne) main chain of **3** is known to luminesce in the similar spectral region.<sup>16,37</sup> The AIE effect was more striking in this system: the emission of the nanoaggregates of **3** was ~46 times more efficient than that of its molecularly dissolved species.

The picture now becomes clear: in the aggregation state, **1** is virtually nonluminescent, **2** emits moderately, and **3** is a most efficient emitter. It is well-known that a stiff polymer backbone distorts the packing of its mesogenic pendants.<sup>15,16,25,38,39</sup> The rigid polyacetylene backbone of **1** may not allow its directly attached silole pendants to pack well in the aggregation state, thus

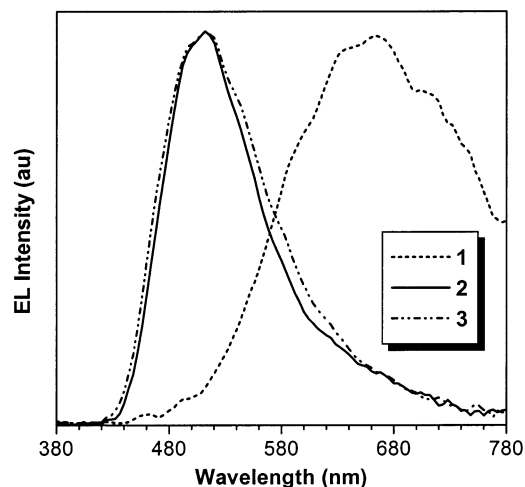


**Figure 7.** Electroluminescence spectra of single-layer devices of **1** (Table 1, no. 6), **2** (Table 2, no. 1), and **3** (Table 2, no. 4) with a device configuration of ITO/polymer/LiF/Al.

making the polymer AIE-inactive. The long flexible spacer of nonanyloxy group decouples the silole pendants of **2** and **3** from their polyacetylene backbone and enables the silole groups to pack in a more regular fashion, hence making the polymers AIE-active. The emitting center changes with the molecular structure of the polymer: **1** emits from its polyacetylene backbone, **2** from its silole pendants, and **3** from its backbone and pendants. This double emission makes **3** the best emitter among the three polymers.

We checked the EL performances of the polymer thin films, using a single-layer device configuration. The EL spectrum of **1** peaked at 664 nm, while the emission maxima of **2** and **3** were at ~512 nm (Figure 7). All the EL devices exhibited similarly low current efficiencies: 0.014 (**1**), 0.013 (**2**), and 0.013 cd/A (**3**). The EL data clearly contradict with the PL data discussed above, suggesting that the device configuration is far from optimized. One possible cause for the inferior performance is the unbalanced charge injection and transport in the single-layer EL devices. We thus tried to modify the device configuration, using **3**, the most PL-active polymer, as the emitting material. We added PVK, one of the best-known hole-transport polymers, and Al(q)<sub>3</sub>, a very widely used electron-transport material, on the anode and cathode sides, respectively, to facilitate the charge injection and to enhance the charge-transport efficiencies in the EL device. Between the PVK and Al(q)<sub>3</sub> layers, we added a layer of BCP, a hole-blocking material, to prevent the holes from traveling through to reach the cathode. With these modifications, an EL device with a configuration of ITO/(**3**:PVK)(1:4)/BCP/Al(q)<sub>3</sub>/LiF/Al was fabricated, whose performance was greatly improved, in comparison to its single-layer counterpart. The multilayer device emitted a blue light of 496 nm with a maximum brightness of 1118 cd/m<sup>2</sup>. The emission peak is 16 nm blue-shifted from its PL maximum, probably due to the dilution effect by the polymer matrix, as reported in our early communication,<sup>5</sup> and/or by the microcavity effect proposed by other researchers.<sup>40</sup> The maximum CE and  $\eta_{EL}$  of the device were 1.45 cd/A (Figure 8) and 0.55%, respectively, which are comparable to some of the best results reported by other research groups for blue-emitting LEDs.<sup>41</sup>

**Restricted Intramolecular Twisting.** The AIE effect is of technological implications, considering that

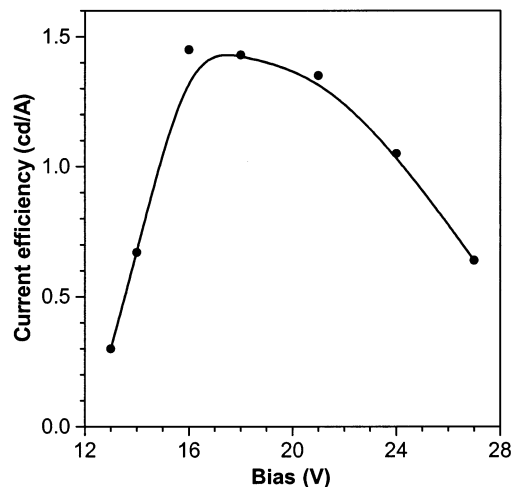


**Figure 8.** Current efficiency vs. applied bias in a multilayer electroluminescence device of **3** (sample from Table 2, no. 4) with a device configuration of ITO/(**3**:PVK)(1:4)/BCP/Al(q)<sub>3</sub>/LiF/Al, where PVK = poly(9-vinylcarbazole), BCP = bathocuproine, and Al(q)<sub>3</sub> = tris(8-hydroxyquinolino)aluminum.

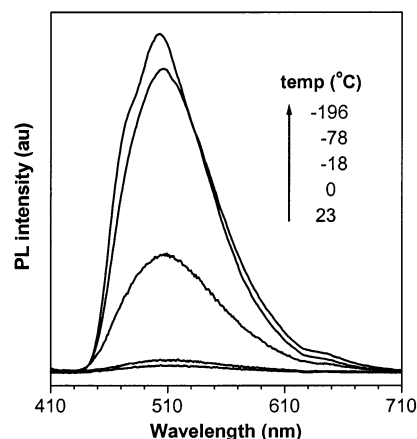


**Figure 9.** Photoluminescence spectra of a dioxane solution of **3** (Table 2, no. 4) with a concentration of 10  $\mu$ M at different temperatures. Excitation wavelength: 407 nm.

all organic and polymeric light-emitting materials are used as solid films in their LED applications. Aggregation normally quenches light emission;<sup>17</sup> what is then the cause for this “abnormal” AIE phenomenon? To address this mechanistic question, we designed and carried out more experiments. We chose dioxane, a common solvent with a “high” melting point (mp = 11.8 °C) that readily solidifies with a small extent of cooling from room temperature. When a dilute dioxane solution of **3** (10  $\mu$ M) was cooled, the intensity of its PL spectrum was increased (Figure 9). The spectral profile hardly changed with temperature, suggesting that the emission is still associated with the radiative decay of the singlet excitons<sup>7a</sup> but not their triplet cousins. The peak intensity of the PL spectrum changed with temperature in a nonlinear fashion (Figure 10). When cooled from 23 °C (room temperature) to below the mp of the solvent, the liquid solution changed to a solid “glass”. The intramolecular rotations or twistings of the peripheral phenyl rings upon the axes of the single bonds linked to the central silacyclopentadiene cores may be physically restricted by the solid environmental surroundings. This restricted rotation in some sense rigidifies the chromophoric molecule as a whole, thus making the silole pendant more emissive. The PL intensity was progres-

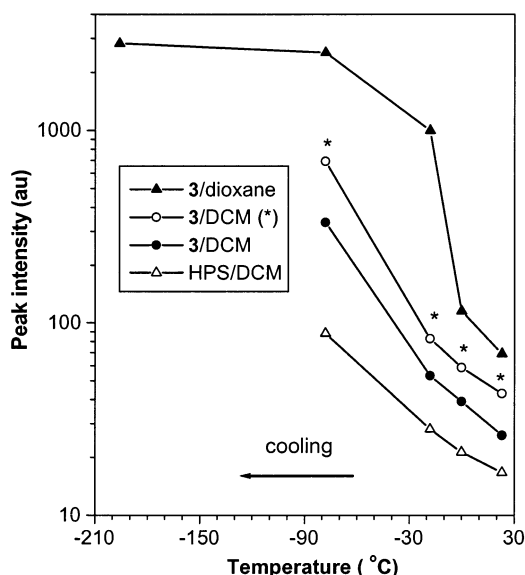


**Figure 10.** Effect of temperature on peak intensity of the photoluminescence spectra of **3** in dioxane and DCM. Data for HPS are shown for comparison. Excitation wavelength: 407 nm. All the solutions have a concentration of  $10 \mu\text{M}$  except for the one marked with an asterisk, whose concentration is  $20 \mu\text{M}$ .

sively increased when the temperature was successively decreased from  $+23$  to  $-78$  °C, indicating that the cooling is gradually limiting the thermally induced or activated intramolecular rotations. Further decreasing the temperature from  $-78$  to  $-196$  °C caused little change in the peak intensity, implying that the intramolecular rotations have almost completely frozen at  $-78$  °C.

To separate the cooling effect from the “glass” effect, we chose DCM, a liquid with a high solvation power but a low melting point, which can keep both the solvent and the solute in the solution state during the cooling process. The peak intensity of the PL spectrum of a dilute DCM solution of **3** ( $10 \mu\text{M}$ ) at room temperature was weaker than that of the dioxane solution, due to the stronger solvating power of DCM to the polymer. The PL intensity of the solution increased with a decrease in temperature in a nearly “linear” fashion (in the semilog plot). This enhancement in emission must be due to the restricted intramolecular rotation caused by cooling-induced conformation freezing because the melting point of the solvent ( $-95$  °C) is lower than the lowest temperature we tested for this solution ( $-78$  °C). The solvent should be in the liquid state, and the solute should be molecularly dissolved at all the temperatures tested. We doubled the solution concentration to  $20 \mu\text{M}$  and found that the emission enhancements were also roughly doubled at all the temperatures (data marked with an asterisk in Figure 10). This once again proves that the solute has indeed remained molecularly dissolved at the low temperatures because if the solute aggregates, it should evoke a clear “nonlinear” response (in the semilog scale) to the concentration change. We used a dilute DCM solution of HPS ( $10 \mu\text{M}$ ) as a control and found that the silole compound also exhibited an approximately linear semilog relationship between the increase in PL intensity and the decrease in temperature. Noting that HPS is highly soluble in DCM, the high PL intensities at the low temperatures should be beyond doubt caused by the restricted intramolecular rotation or twisting. The PL intensities of the HPS/DCM

solution were lower than those of the **3**/DCM solution with the same concentration; this may be partially caused by the even higher solvating power of the solvent to the low molecular weight silole compound.

Twisted intramolecular charge transfer (TICT) has been found to greatly alter luminescence properties of some chromophoric molecules containing donor and acceptor groups, with off-on manipulations of light emission (from nonluminescent “off” to luminescent “on” state) achieved in certain systems.<sup>42,43</sup> Since silole is not such a push–pull chromophore, the TICT effect may not be at play in our system. It is known that torsional or rotational energy relaxation can nonradiatively deactivate excited molecules.<sup>44,45</sup> Restriction of the rotational or twisting movement will block the radiationless channel and populate the radiative decay of the excitons. The rigid chain of **1** may not allow its silole pendants to pack well and the large free volumes in the nanoaggregates may still enable the intramolecular rotations of the phenyl-silole single bonds to occur; the polymer thus remained nonemissive even in its aggregation state. We have recently found that the aggregates of our hyperbranched silole polymers are also nonluminescent, probably due to the same reasons: the poor packing of the silole groups in the nanoaggregates and the easy intramolecular rotation or twisting in the large void spaces in the hyperbranched polymers. Cooling the polymer solutions can, however, enhance their emission efficiencies.<sup>46</sup> This further supports our hypothesis that the underlying reason for the AIE phenomenon observed in linear silole polymers **2** and **3** is the restricted intramolecular rotation or twisting in the well packed silole nanoaggregates. A recent paper reported that restricting the rotation or twisting of the single bond between two neighboring thienyl rings could lead to a big increase (up to 12 times) in the emission efficiency of polythiophenes.<sup>47</sup> Thus, the restricted intramolecular rotation does not only work for our linear silole polymers but also may find applications in enhancing light emissions of other chromophoric systems.

### Concluding Remarks

In this work, we synthesized a group of new silolylacetylene polymers and studied their light-emitting properties. Our main results and key findings can be summarized as follows:

We successfully developed a new synthetic route for the preparation of silole polymers, which produced high molecular weight polysilolylacetylenes in high yields. Overcoming the involved synthetic difficulties, we accomplished the polymerizations of silolylacetylene monomers **10–12** using  $\text{NbCl}_5$ - and  $\text{WCl}_6$ - $\text{Ph}_4\text{Sn}$  as catalysts. Monomer **10** is the first example of a monosubstituted acetylene with a directly attached silyl group that can be successfully polymerized by the Nb catalyst, while **11** and **12** represent the first siloxyacetylenes that can be polymerized by the W catalyst. All the polymerizations yielded completely soluble polymers of high thermal stability.

The molecular structures of the polymers greatly affected their optical properties. The direct electronic communication between the polyacetylene backbone and the silole pendants of **1** provided the polymer with a better conjugation and enabled efficient energy transfer from the side groups to the main chain. The polyacetylene backbone of **1** emitted faintly in the red spectral region, in agreement with the early finding that (un-

substituted) polyacetylene is virtually nonluminescent. The long nonanyloxy spacers electronically decoupled the silole pendants of **2** from its polyacetylene backbone and the segregated silole rings acted as the emitting centers in the polymer nanoaggregates because the poly-(1-alkyne) backbone is not an active chromophore.<sup>15,16</sup> Polymer **3** was more emissive because the excitons of the silole pendants and the poly(phenylalkyne) backbone both undergo radiative transitions in the similar spectral region.<sup>37–39</sup>

The AIE effect was not operative in polymer **1** because the silole pendants directly attached to the rigid polyacetylene backbone cannot pack well in the aggregation state and the large free volumes still permit the phenyl–silole bonds to undergo intramolecular rotation. The decoupling of the silole pendants of **2** and **3** from their polyacetylene backbones by the flexible nonanyloxy spacers allowed the pendants to pack well in the aggregation state, enabling the AIE effect to function in the nanoaggregates and solid films. Up to ~46 times enhancement in the emission efficiency was induced by the aggregate formation.

The light emission could be enhanced not only by adding poor solvents to induce nanoaggregate formation but also by cooling the molecularly dissolved solutions to restrict the intramolecular rotation. The changes in the emission efficiency caused by changing solvent and temperature may respectively be regarded as special kinds of solvato- and thermochromisms,<sup>5,48</sup> offering versatile means to manipulate the light emission of the conjugated polymers by simple external stimuli.

The EL performance of **3** was improved by modifying its device configuration. Its multilayer device emitted a blue light of 496 nm with a maximum brightness of 1118 cd/m<sup>2</sup>. The device efficiencies of 1.45 cd/A (CE) and 0.55% ( $\eta_{EL}$ ) are the best results reported so far for polyacetylene-based EL devices,<sup>37</sup> which may be further improved by modifying the molecular structure of the polymers and by optimizing the configuration of the EL devices. Work along this line is currently in progress in our laboratories.

**Acknowledgment.** The work described in this paper was partially supported by the Research Grants Council of Hong Kong through Grants HKUST 6187/99P, 6121/01P, and 6085/02P. This project also benefited from the financial support of the University Grants Committee (Hong Kong) under an Area of Excellence Scheme (Project No. AoE/P-10/01-1-A). We sincerely thank Prof. K. S. Wong of the Department of Physics of our University for his helpful discussions.

**Supporting Information Available:** Text giving details about the reagents (materials), instrumentation procedures, device fabrications, monomer syntheses, and polymerization reactions and detailed characterization data for all the new monomers and polymers, including their isolation yields, physical forms (colors), molecular weights, and spectroscopic data (IR, <sup>1</sup>H and <sup>13</sup>C NMR, MS, and UV), and figures showing IR and <sup>13</sup>C NMR spectra of **11** and **2**, TGA thermograms of **1–3**, photoluminescence spectra of **2**, and a plot of the quantum yield of **2**. This material is available free of charge via the Internet at <http://pubs.acs.org>.

## References and Notes

- (1) For reviews, see: (a) Lee, V. Y.; Sekiguchi, A.; Ichinohe, M.; Fukaya, N. *J. Organomet. Chem.* **2000**, *611*, 228–235. (b) Hermanns, J.; Schmidt, B. *J. Chem. Soc., Perkin Trans. 1* **1999**, 81–102. (c) Yamaguchi, S.; Tamao, K. *J. Chem. Soc., Dalton Trans.* **1998**, 3693–3702.
- (2) (a) Yamaguchi, S.; Tamao, K. *Bull. Chem. Soc. Jpn.* **1996**, *69*, 2327–2334. (b) Chuit, C.; Corriu, R. J. P.; Reye, C.; Young, J. C. *Chem. Rev.* **1993**, *93*, 1371–1448.
- (3) An electron mobility as high as  $2 \times 10^{-4}$  cm<sup>2</sup>/(V s) has been reported for a silole molecule 2,5-bis(2,2'-bipyridin-6-yl)-1,1-dimethyl-3,4-diphenylsilole at an electrical strength of 640 kV/cm: (a) Murata, H.; Malliaras, G. G.; Uchida, M.; Shen, Y.; Kafafi, Z. H. *Chem. Phys. Lett.* **2001**, *339*, 161–166. (b) Murata, H.; Kafafi, Z. H.; Uchida, M. *Appl. Phys. Lett.* **2002**, *80*, 189–191.
- (4) (a) Ohshita, J.; Kai, H.; Takata, A.; Iida, T.; Kunai, A.; Ohta, N.; Komaguchi, K.; Shiotani, M.; Adachi, A.; Sakamaki, K.; Okita, K. *Organometallics* **2001**, *20*, 4800–4805. (b) Yamaguchi, S.; Endo, T.; Uchida, M.; Izumizawa, T.; Furukawa, K.; Tamao, K. *Chem.—Eur. J.* **2000**, *6*, 1683–1692.
- (5) (a) Luo, J.; Xie, Z.; Lam, J. W. Y.; Cheng, L.; Chen, H.; Qiu, C.; Kwok, H. S.; Zhan, X.; Liu, Y.; Zhu, D.; Tang, B. Z. *Chem. Commun.* **2001**, 1740–1741. (b) Freemantle, M. *Chem. Eng. News* **2001**, *79* (41), 29.
- (6) Tang, B. Z.; Zhan, X.; Yu, G.; Lee, P. P. S.; Liu, Y.; Zhu, D. *J. Mater. Chem.* **2001**, *11*, 2874–2978.
- (7) Chen, H. Y.; Lam, J. W. Y.; Luo, J. D.; Ho, Y. L.; Tang, B. Z.; Zhu, D. B.; Wong, M.; Kwok, H. S. *Appl. Phys. Lett.* **2002**, *81*, 774–576.
- (8) The highest  $\eta_{EL}$  possible for a singlet emitter has been theoretically predicted to be ~5.5%, but recent research in the area suggests that this limit may be uplifted to ~9%.<sup>9</sup>
- (9) (a) Cao, Y.; Parker, I. D.; Yu, G.; Zhang, C.; Heeger, A. J. *Nature (London)* **1999**, *397*, 414–417. (b) Kim, J. S.; Ho, P. K.; Greenham, N. C.; Friend, R. H. *J. Appl. Phys.* **2000**, *88*, 1073–1081.
- (10) Configuration of the EL device: ITO/CuPc/TPD/HPS/Al(q)<sub>3</sub>/LiF/Al, where ITO = indium tin oxide, CuPc = copper phthalocyanine, TPD = N,N'-diphenyl-N,N'-bis(3-methylphenyl)-1,1'-diphenyl-4,4'-diamine, and Al(q)<sub>3</sub> = tris(8-hydroxyquinolato)aluminum.
- (11) Ohshita, J.; Kai, H.; Sumida, T.; Kunai, A.; Adachi, A.; Sakamaki, K.; Okita, K. *J. Organomet. Chem.* **2002**, *642*, 137–142.
- (12) Ktaft, A.; Grimsdale, A. C.; Holmes, A. B. *Angew. Chem., Int. Ed.* **1998**, *37*, 402–428.
- (13) (a) Adachi, A.; Yasuda, H.; Sanji, T.; Sakurai, H.; Okita, K. *J. Lumin.* **2000**, *87–9*, 1174–1176. (b) Woo, H. G.; Song, S. J.; Kim, B. H.; Yun, S. S. *Mol. Cryst. Liq. Cryst.* **2000**, *349*, 87–90. (c) Tamao, K.; Yamaguchi, S.; Shiozaki, M.; Nakagawa, Y.; Ito, Y. *J. Am. Chem. Soc.* **1992**, *114*, 5867–5869. (d) Yamaguchi, S.; Goto, T.; Tamao, K. *Angew. Chem., Int. Ed.* **2000**, *39*, 1695–1697. (e) Lee, Y.; Sadki, S.; Tsuie, B.; Reynolds, J. R. *Chem. Mater.* **2001**, *13*, 2234–2236. (f) Corriu, R. J.-P.; Douglas, W. E.; Yang, Z.-X. *J. Organomet. Chem.* **1993**, *456*, 35–39. (g) Oshita, J.; Hamaguchi, T.; Toyoda, E.; Kunai, A.; Ishikawa, M.; Naka, A. *Organometallics* **1999**, *18*, 1717–1723. (h) Toyoda, E.; Kunai, A.; Ishikawa, M. *Organometallics* **1995**, *14*, 1089–1091. (i) Sanji, T.; Sakai, T.; Kabuto, C.; Sakurai, H. *J. Am. Chem. Soc.* **1998**, *120*, 4552–4553. (j) Yamaguchi, S.; Jin, R.-Z.; Itami, Y.; Goto, T.; Tamao, K. *J. Am. Chem. Soc.* **1999**, *121*, 10420–10421.
- (14) Ivin, K. J.; Mol, J. C. *Olefin Metathesis and Metathesis Polymerization*; Academic Press: San Diego, CA, 1997.
- (15) (a) Mi, Y.; Tang, B. Z. *Polym. News* **2001**, *26*, 170–176. (b) Lam, J. W. Y.; Kong, X.; Dong, Y. P.; Cheuk, K. K. L.; Xu, K.; Tang, B. Z. *Macromolecules* **2000**, *33*, 5027–5040. (c) Kong, X.; Tang, B. Z. *Chem. Mater.* **1998**, *10*, 3352–3363. (d) Tang, B. Z.; Kong, X.; Wan, X.; Peng, H.; Lam, W. Y.; Feng, X.; Kwok, H. S. *Macromolecules* **1998**, *31*, 2419–2432.
- (16) (a) Lam, J. W. Y.; Dong, Y. P.; Cheuk, K. K. L.; Luo, J. D.; Xie, Z. L.; Kwok, H. S.; Mo, Z. S.; Tang, B. Z. *Macromolecules* **2002**, *35*, 1229–1240. (b) Huang, Y. M.; Ge, W.; Lam, J. W. Y.; Tang, B. Z. *Appl. Phys. Lett.* **2001**, *78*, 1652–1654. (c) Tang, B. Z.; Xu, H.; Lam, J. W. Y.; Lee, P. P. S.; Xu, K.; Sun, Q.; Cheuk, K. K. L. *Chem. Mater.* **2000**, *12*, 1446–1455. (d) Huang, Y. M.; Lam, J. W. Y.; Cheuk, K. K. L.; Ge, W.; Tang, B. Z. *Macromolecules* **1999**, *32*, 5976–5978.
- (17) (a) An, B.-K.; Kwon, S.-K.; Jung, S.-D.; Park, S. Y. *J. Am. Chem. Soc.* **2002**, *124*, 14410–14415. (b) Chen, S. H.; Su, A. C.; Huang, Y. F.; Su, C. H.; Peng, G. Y.; Chen, S. A. *Macromolecules* **2002**, *35*, 4229–4232. (c) Deans, R.; Kim, J.; Machacek, M. R.; Swager, T. M. *J. Am. Chem. Soc.* **2000**, *122*, 8565–8566. (d) Zhang, X. J.; Shetty, A. S.; Jenekhe, S. A. *Macromolecules* **1999**, *32*, 7422–7429.

- (18) *Thin Films: Structure and Morphology*; Moss, S. C., Ed.; Materials Research Society: Pittsburgh, PA, 1997.
- (19) Curtis, M. D. *J. Am. Chem. Soc.* **1969**, *91*, 6011–6018.
- (20) Braye, E. H.; Hubel, W.; Caplier, I. *J. Am. Chem. Soc.* **1961**, *83*, 4406–4413.
- (21) Gilman, H.; Cottis, S. G.; Atwell, W. H. *J. Am. Chem. Soc.* **1964**, *86*, 1596–1599.
- (22) Tolane could be eluted much faster than the siloles using hexane/chloroform or chloroform/acetone mixtures as eluents.
- (23) Chen, J.; Law, C. C. W.; Lam, J. W. Y.; Dong, Y.; Lo, S. M. F.; Williams, I. D.; Tang, B. Z. Unpublished results.
- (24) For selected recent reviews, see: (a) Yashima, E. *Anal. Sci.* **2002**, *18*, 3–6. (b) Tang, B. Z. *Polym. News* **2001**, *26*, 262–272. (c) Nagai, K.; Masuda, T.; Nakagawa, T.; Freeman, B. D.; Pinnau, Z. *Prog. Polym. Sci.* **2001**, *26*, 721–798. (d) Tang, B. Z.; Cheuk, K. K. L.; Salhi, F.; Li, B. S.; Lam, J. W. Y.; Cha, J. A. K.; Xiao, X. D. *ACS Symp. Ser.* **2001**, *812*, 133–148. (e) Choi, S. K.; Gal, Y. S.; Jin, S. H.; Kim, H. K. *Chem. Rev.* **2000**, *100*, 1645–1681. (f) Tang, B. Z.; Xu, K.; Sun, Q.; Lee, P. P. S.; Peng, H.; Salhi, F.; Dong, Y. *ACS Symp. Ser.* **2000**, *760*, 146–164.
- (25) (a) Tang, B. Z.; Poon, W. H.; Leung, S. M.; Leung, W. H.; Peng, H. *Macromolecules* **1997**, *30*, 2209–2212. (b) Tang, B. Z.; Kong, X.; Wan, X.; Feng, X.-D. *Macromolecules* **1998**, *31*, 7118. (c) Tang, B. Z.; Kong, X.; Wan, X.; Feng, X.-D. *Macromolecules* **1997**, *30*, 5620–5628. (d) Kong, X.; Lam, J. W. Y.; Tang, B. Z. *Macromolecules* **1999**, *32*, 1722–1730.
- (26) (a) Voronkov, M. G.; Pukhnarevich, V. B.; Sushchinskaya, S. P.; Annenkova, V. Z.; Annenkova, V. M.; Andreeva, N. J. *J. Polym. Sci., Polym. Chem. Ed.* **1980**, *18*, 53–57. (b) Liaw, D. J.; Soum, A.; Fontanille, M.; Parlier, A.; Rudler, H. *Makromol. Chem. Rapid Commun.* **1985**, *6*, 309–313.
- (27) Masuda, T.; Higashimura, T. *Adv. Polym. Sci.* **1987**, *81*, 121–165.
- (28) Xu, K.; Peng, H.; Sun, Q.; Dong, Y.; Salhi, F.; Luo, J.; Chen, J.; Huang, Y.; Zhang, D.; Xu, Z.; Tang, B. Z. *Macromolecules* **2002**, *35*, 5821–5834 and references therein.
- (29) Masuda, T.; Hamano, T.; Tsuchihara, K.; Higashimura, T. *Macromolecules* **1990**, *23*, 1374–1380.
- (30) (a) Masuda, T.; Tang, B. Z.; Tanaka, T.; Higashimura, T. *Macromolecules* **1986**, *19*, 1459–1464. (b) Seki, H.; Tang, B. Z.; Tanaka, A.; Masuda, T. *Polymer* **1994**, *35*, 3456–3462.
- (31) Ginsburg, E. J.; Gorman, C. B.; Grubbs, R. H. In *Modern Acetylene Chemistry*; Stang, P. J., Diederich, F., Eds.; VCH: New York, 1995; Chapter 10, pp 353–383.
- (32) Kunzler, J.; Percec, V. *J. Polym. Sci., Polym. Chem. Ed.* **1990**, *28*, 1221–1236.
- (33) *Optical Properties of Nanoparticles*; Trager, F., Ed.; Springer-Verlag: Berlin, 2001.
- (34) (a) Tang, B. Z.; Xu, H. *Macromolecules* **1999**, *32*, 2569–2576. (b) Tang, B. Z.; Peng, H.; Leung, S. M.; Au, C. F.; Poon, W. H.; Chen, H.; Wu, X.; Fok, M. W.; Yu, N.-T.; Hiraoka, H.; Song, C.; Fu, J.; Ge, W.; Wong, K. L. G.; Monde, T.; Nemoto, F.; Su, K. C. *Macromolecules* **1998**, *31*, 103–108. (c) Tang, B. Z.; Leung, S. M.; Peng, H.; Yu, N.-T.; Su, K. C. *Macromolecules* **1997**, *30*, 2848–2852.
- (35) Suspensions of maghemite particles with sizes of a few tens of nanometers in chloroform and water exhibited little scattering-induced optical losses and showed “normal” absorption spectra. (a) Tang, B. Z.; Geng, Y.; Lam, J. W. Y.; Li, B.; Jing, X.; Wang, X.; Wang, F.; Pakhomov, A. B.; Zhang, X. *Chem. Mater.* **1999**, *11*, 1581–1589. (b) Tang, B. Z. *CHEMTECH* **1999**, *29* (11), 7–12. (c) Tang, B. Z.; Geng, Y.; Sun, Q.; Zhang, X. X.; Jing, X. *Pure Appl. Chem.* **2000**, *72*, 157–162.
- (36) Huang, Y. M.; Ge, W.; Lam, J. W. Y.; Tang, B. Z. *Appl. Phys. Lett.* **1999**, *75*, 4094–4096.
- (37) (a) Hidayat, R.; Fujii, A.; Ozaki, M.; Teraguchi, M.; Masuda, T.; Yoshino, K. *Synth. Met.* **2001**, *119*, 597–598. (b) Sun, R. G.; Zheng, Q. B.; Zhang, X. M.; Masuda, T.; Kobayashi, T. *Jpn. J. Appl. Phys.* **1999**, *38*, 2017–2023. (c) Wang, Y. Z.; Sun, R. G.; Wang, D. K.; Swager, T. M.; Epstein, A. J. *Appl. Phys. Lett.* **1999**, *74*, 2593–2595.
- (38) (a) Lam, J. W. Y.; Luo, J.; Dong, D.; Cheuk, K. K. L.; Tang, B. Z. *Macromolecules* **2002**, *35*, 8288–8299. (b) Tang, B. Z.; Chen, H. Z.; Xu, R. S.; Lam, J. W. Y.; Cheuk, K. K. L.; Wong, H. N. C.; Wang, M. *Chem. Mater.* **2000**, *12*, 213–221. (c) Kong, X.; Wan, X.; Kwok, H. S.; Feng, X.-D.; Tang, B. Z. *Chin. J. Polym. Sci.* **1998**, *16*, 185–192.
- (39) (a) Tang, B. Z.; Lam, J. W. Y.; Luo, J. D.; Dong, Y.; Cheuk, K. K. L.; Xie, Z.; Kwok, H.-S. *Proc. SPIE* **2001**, *4463*, 132–138. (b) Tang, B. Z.; Lam, J. W. Y.; Kong, X.; Salhi, F.; Cheuk, K. K. L.; Kwok, H. S.; Huang, Y. M.; Ge, W. *Proc. SPIE* **2000**, *4107*, 24–30. (c) Tang, B. Z.; Lam, J. W. Y.; Kong, X.; Lee, P. P. S.; Wan, X.; Kwok, H. S.; Huang, Y. M.; Ge, W.; Chen, H.; Xu, R.; Wang, M. *Proc. SPIE* **1999**, *3800*, 62–71.
- (40) Bulovic, V.; Khalfin, V. B.; Gu, G.; Burrows, P. E.; Garbuzov, D. Z.; Forrest, S. R. *Phys. Rev. B* **1998**, *58*, 3730–3740.
- (41) Some of the best blue-emitting LEDs have exhibited maximum CE and  $\eta_{EL}$  values of 2.1 cd/A and 1.3%, respectively: (a) Rees, I. D.; Robinson, K. L.; Holmes, A. B.; Towns, C. R.; O'Dell, R. *MRS Bull.* **2002**, *27*, 451. (b) Palilis, L. C.; Lidzey, D. G.; Redecker, M.; Bradley, D. D. C.; Inbasekaran, M.; Woo, E. P.; Wu, W. W. *Synth. Met.* **2001**, *121*, 1729–1730. (c) Jiang, X. Z.; Liu, S.; Ma, H.; Jen, A. K. Y. *Appl. Phys. Lett.* **2000**, *76*, 1813–1815.
- (42) Rettig, W.; Baumann, W. In *Progress in Photochemistry and Photophysics*; Rabek, J. F., Ed.; CRC Press: Boca Raton, FL, 1990; Vol. 6, Chapter 3, pp 79–134.
- (43) (a) Morozumi, T.; Anada, T.; Nakamura, H. *J. Phys. Chem. B* **2001**, *105*, 2923–2931. (b) Soujanya, T.; Fessenden, R. W.; Samanta, A. *J. Phys. Chem.* **1996**, *100*, 3507–3512.
- (44) (a) Rabek, J. F. *Mechanisms of Photophysical Processes and Photochemical Reactions in Polymers: Theory and Applications*; Wiley: New York, 1987. (b) *Photonic Polymer Systems*; Wise, D. L.; Wnek, G. E.; Trantolo, D. J.; Cooper, T. M.; Gresser, J. D., Eds.; Marcel Dekker: New York, 1998.
- (45) (a) Wang, P. F.; Wu, S. K. *J. Lumin.* **1994**, *62*, 33–39. (b) Wong, K. S.; Wang, H.; Lanzani, G. *Chem. Phys. Lett.* **1998**, *288*, 59–64. (c) Wong, K. S. Personal communication.
- (46) Chen, J.; Law, C. C. W.; Lam, J. W. Y.; Tang, B. Z. Unpublished results.
- (47) Li, Y.; Vamvounis, G.; Holdcroft, S. *Macromolecules* **2002**, *35*, 6900–6906.
- (48) For a multigraph, see: *An Introduction to Molecular Electronics*; Petty, M. C., Bryce, M. R., Bloor, D., Eds.; Edward Arnold: London, 1995.

MA0213504